Asian Journal of Chemistry; Vol. 27, No. 3 (2015), 837-840

ASIAN JOURNAL OF CHEMISTRY

http://dx.doi.org/10.14233/ajchem.2015.17490

Theoretical Study on the Charge Transport Property of Thia- or Selenadiazole Compound

SHAN-SHAN ZHAO[1], DONG-HUA HU[1,*] and TIE-CHAO JIANG[2,*]

[1]Medicinal Materials Synthesis and Design Lab, ChangChun University of Chinese Medicine, Changchun, Jilin, 130117, P.R. China
[2]China-Japan Union Hospital of Jilin University, Jilin University, Changchun, Jilin, 130033, P.R. China

*Corresponding authors: E-mail: zhaoss778@nenu.edu.cn

Received: 1 March 2014; *Accepted*: 19 May 2014; *Published online*: 19 January 2015; AJC-16681

In this work, we carried out theoretical investigation on the charge-transporting nature of 4,11-*bis*-[(triisopropylsilanyl)-ethynyl]-2-thia-1,3-diaza-cyclopenta[*b*]anthracene (**1**) and 4,11-*bis*-[(triisopropylsilanyl)-ethynyl]-2-selena-1,3-diaza-cyclopenta[*b*]anthracene (**2**) by Marcus theory and first-principle band structure. The character of the frontier molecular orbitals, reorganization energies, transfer integrals and band structures are considered in detail. The results show that the compounds **1** and **2** are ambipolar material, both electron and hole are favor of transporting. The intermolecular π-π ineraction and S···N/Se···N interaction provide the holes and electrons transport channels. The introduction of Se atom can effectively reduce the reorganization energy and considerably improve the electron transfer integrals, thus **2** is found to be a good candidate for ambipolar semiconducting material with high mobility and balanced transport.

Keywords: DFT, Marcus theory, Band structure.

INTRODUCTION

Organic semiconductors have received tremendous attention in recent years because of their potential application in organic light emitting diodes (OLED), organic solar cells and organic field-effect transistors (OFETs)[1-3]. Previous investigations demonstrate that designing of molecules with chalcogen atoms is a viable strategy to create organic semiconductors[4-6]. Lindner *et al.*[7] reported the synthesis and solid-state properties of S-containing (aza) diazoles (**1**) and Se-containing (aza) diazoles (**2**) as shown in Fig. 1. In crystals, the S-N and Se-N interaction as the supramolecular motif drive the effective self-assembly and enforce compulsory head-to-head packing. Recently, theoretical study can well explain and predict the charge mobility of compound[8,9]. In order to gain insight into the charge transfer property of compounds **1** and **2**, its charge transport features were systematically investigated by Marcus theory and band model calculation in this article.

COMPUTATIONAL METHODS

The ground state and cationic state structures of compounds **1** and **2** were fully optimized at density functional theory level with B3LYP functional and 6-31 + g** basis set using G09 package. Harmonic vibrational frequencies were also calculated and confirmed that each optimized configuration was a minimum on the potential energy surface.

To describe the charge-transport properties of compound, the charge hopping model, described by the Marcus electron transfer model[10] was employed. In this model, charge carrier diffuse by hopping from a charge molecule to an adjacent neutral one and each hopping step has been considered as a non-adiabatic electron-transfer reaction involving a self-exchange charge between neighboring molecules. Thus the rate of charge transfer between neighboring molecules, k can be expressed as:

$$k = \frac{4\pi^2}{h}\frac{1}{\sqrt{4\pi\lambda k_B T}}\beta^2 \exp\left(-\frac{\lambda}{4k_B T}\right) \quad (1)$$

Here, V is the intermolecular transfer integral, λ is the reorganization energy, h = h/2π, h is the Planck constant. k_B is the Boltzmann constant and T is the temperature.

The charge mobility can be evaluated from the Einstein relation:

$$D = \frac{1}{2n}\sum_i r_i^2 k_i P_i \quad (2)$$

$$P_i = k_i / \sum_i k_i \quad (3)$$

Here n = 3 is the dimensionality, i is the all nearest adjacent molecules, d_i, k_i, p_i are the corresponding center-to-center hopping distance, hopping rate and the hopping probability due to the charge carrier to the ith neighbor, respectively. Using eqn. 1-3, the carrier mobility can be calculated.

RESULTS AND DISCUSSION

Geometric sturcture and molecular orbital: The schematic structures of **1** and **2** with the number of some key atom are shown in Fig. 1. The main geometrical parameters optimized at B3LYP level and the experimental results determined by the single-crystal X-ray diffraction are listed in Table-1. Since the charge transport property is closely related to the Frontier molecular orbitals (FMOs), especially HOMO and LUMO, we show the FMOs in Fig. 2. The results indicate that both HOMO and LUMO for **1** and **2** possess π-orbital features and spread over the whole compound, which are facilitate to the charge transport. Compounds **1** and **2** show similar electron density distribution on the FMOs. The π-orbital of S and Se atom primarily contribute to the LUMO and less to the HOMO.

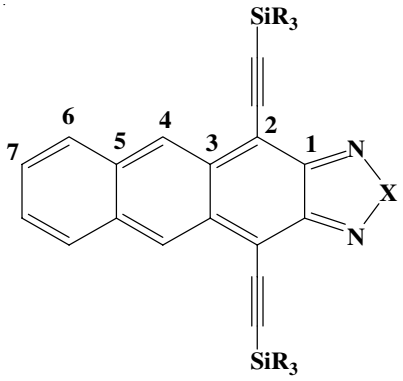

Fig. 1. Molecular structure

Reorganization energy: Reorganization energy is one key parameter in governing the hopping rate. Here, the intramolecular reorganization energies of **1** and **2** are evaluated from adiabatic potential-energy surfaces based on B3LYP/6-31+G** level. The calculated reorganization energies are listed in Table-2. The results show that the hole and electron reorganization energies of compounds **1** and **2** are small, which might lead to ambipolar transport behaviour. Both hole and electron reorganization energies of **2** are smaller than that of **1**, revealing that the introduction of Se can effectively reduce the reorganization energy and then should improve the charge transfer behaviour. In order to illustrate the diversity of reorganization

TABLE- 2
INTRAMOLECULAR ELECTRON REORGANIZATION ENERGIES λ (IN eV) CALCULATED FROM THE ADIABATIC POTENTIAL-ENERGY SURFACES OF NEUTRAL/CATION OR NEUTRAL/ANION SPECIES, DIFFUSION COEFFICIENT D (cm^2/s), AND THE ELECTRON MOBILITY μ (cm^2/Vs) OF COMPOUNDS **1** AND **2**

Compound		λ (eV)	D ($E^{-2}*d^{-2}cm^2/s$)	μ (cm^2/Vs)
1	Hole	0.172	0.202	7.814
	Electron	0.221	0.073	2.834
2	Hole	0.165	0.208	8.027
	Electron	0.205	0.119	4.591

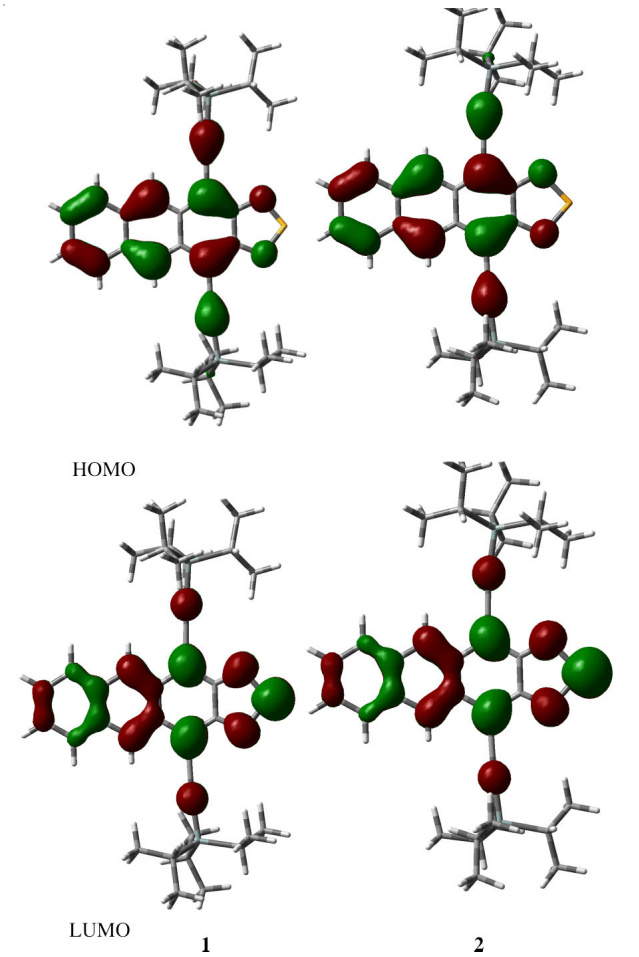

Fig. 2. Frontier molecular orbitals calculated at B3LYP wave function

TABLE-1
SELECTED BOND LENGTHS (Å) IN THE GROUND AND CATIONIC STATE BASED ON B3LYP/6-31+g** LEVEL

Bond length (Å)	1				2			
	Ground (S_0)	Cationic ($^+$S)	Anionic ($^-$S)	X-ray	Ground (S_0)	Cationic ($^+$S)	Anionic ($^-$S)	X-ray
S/Se-N	1.631	1.638	1.667	1.610	1.781	1.786	1.815	1.784
C_1-N	1.350	1.338	1.340	1.364	1.339	1.329	1.335	1.331
C_1-C_2	1.417	1.435	1.424	1.402	1.423	1.438	1.425	1.423
C_2-C_3	1.427	1.434	1.442	1.425	1.423	1.432	1.439	1.410
C_3-C_4	1.413	1.404	1.403	1.408	1.414	1.403	1.403	1.404
C_4-C_5	1.391	1.404	1.405	1.386	1.390	1.405	1.404	1.375
C_5-C_6	1.436	1.423	1.428	1.433	1.436	1.423	1.428	1.428
C_6-C_7	1.368	1.379	1.378	1.348	1.367	1.379	1.377	1.350
C_1-C_1'	1.455	1.445	1.465	1.432	1.465	1.456	1.475	1.457
C_3-C_3'	1.461	1.459	1.460	1.442	1.461	1.458	1.458	1.453
C_5-C_5'	1.451	1.443	1.443	1.429	1.452	1.444	1.444	1.449
C_7-C_7'	1.434	1.420	1.424	1.412	1.434	1.420	1.425	1.423

energy and shed some light on structural torsion through the charge transport, we investigate the modifications of geometry parameters induced by hole or electron injection of compounds **1** and **2** as shown in Table-3. The results reveal that the structure distortions are slight, which are consist with the small reorganizatin energy. In the cationic and anionic state, the variation of bond X-N, N-C_1, C_1-C_2 in **2** are smaller than that in **1**, resulting in small λ_h and λ_e. Thus compound **2** should exhibit more excellent ambipolar transport behaviour due to the improvement of hole and electron reorganization energies.

TABLE-3
MODIFICATIONS OF BOND LENGTHS (Å) INDUCED BY HOLE OR ELECTRON INJECTION BASED ON B3LYP/6-31+g** LEVEL

Bond length (Å)	1		2	
	$^{+}S–S_0$	$^{-}S–S_0$	$^{+}S–S_0$	$^{-}S–S_0$
S/Se-N	0.007	0.036	0.005	0.034
C_1-N	-0.012	-0.010	-0.010	-0.004
C_1-C_2	0.018	0.007	0.015	0.002
C_2-C_3	0.007	0.015	0.009	0.016
C_3-C_4	-0.009	-0.010	-0.011	-0.011
C_4-C_5	0.013	0.014	0.015	0.014
C_5-C_6	-0.013	-0.008	-0.013	-0.008
C_6-C_7	0.011	0.010	0.012	0.010
C_1-C_1'	-0.010	0.010	-0.009	0.010
C_3-C_3'	-0.002	-0.001	-0.003	-0.003
C_5-C_5'	-0.008	-0.008	-0.008	-0.008
C_7-C_7'	-0.014	-0.010	-0.014	-0.009

Transfer integral: For conductive materials, the transfer integrals play an important role in determining the charge carrier mobility. Since the magnitudes of transfer integrals are sensitive to the orientation adjacent molecules, it is necessary to understand the molecular stacking arrangements in the crystal. The compounds **1** and **2** exhibit intermolecular π-π stacking structures and head-to-head dimerization in the solid state. The head-to-head dimers are almost plan and form remarkably short intermolecular distance with the S-N or Se-N bond of 2.968 and 2.820 Å, respectively. The main hopping pathways, which have been selected based on the single crystal structure and used to calculate the transfer integrals, are shown in Fig. 3. The other adjacent molecules were not described because of their smaller transfer integrals with relatively long distances. The transfer integrals of hole (V_h) and electron (V_e) calculated with ADF at the PW91/TZP level of theory are listed in Table-4. The results indicate that the magnitudes of transfer integrals are sensitive to the molecular stacking arrangements in crystal. The V_h and V_e for these pathways are big and in the range of 10^{-2}-10^{-1} eV. For the V_h, the parallel pathway 3 for compounds **1** and **2** show the largest values, indicating that the π-π packing in pathway 3 is favorable to the HOMO electronic coupling of neighbors and it improves the hole mobility of material. For the V_e, pathway 2 with π-π interaction for compounds **1** and **2** show the highest values. While in pathway 1 with the short S···N and Se···N for compounds **1** and **2**, the V_e are also large with the values of 95.65 and 154.51 meV respectively, suggesting that S···N and Se···N interaction is favorable to the LUMO electronic coupling between neighbors and plays a major role in the determination of the electron mobility of material. Moreover, the Se···N interaction obviously contribute to larger V_e values than the S···N interaction. Thus

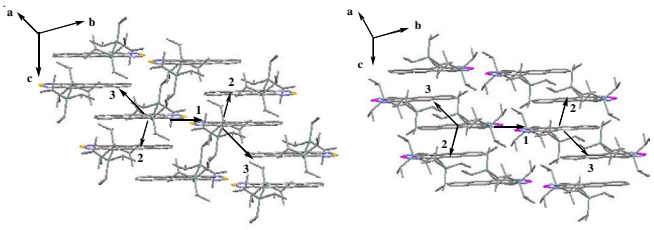

Fig. 3. Main hopping pathways extracted from crystal **1** (a) and **2** (b)

TABLE-4
DIMER CENTER OF MASS (cm) DISTANCE (d, Å) AND THE CALCULATED CHARGE TRANSFER INTEGRALS OF HOLE (V_h, meV) AND ELECTRON (V_e, meV) FOR THE MAJOR PATHWAYS

Compound	Pathway	d (Å)	V_h (meV)	V_e (meV)
1	1	9.182	18.40	95.65
	2	5.941	60.82	187.35
	3	8.049	166.70	84.84
2	1	9.185	30.14	154.51
	2	5.957	40.84	183.32
	3	8.020	159.56	93.43

the Se···N interaction is a supramolecular motif that should drive the effective self-assembly and facilitate electron transport.

Charge mobility: Combining the parameters mentioned above, we estimated the charge mobilities by Marcus charge transfer mode as listed in Table-2. The calculated charge mobility are high and in the range of 1-10 cm^2/Vs. Compound **1** and **2** display ambipolar transporting features with balanced hole mobility and electron mobility. Apparently, the hole and electron mobility for **2** is relatively higher than these for **1**, because of its smaller λ and larger V.

Electronic band structure: The electronic band-structure calculations were performed with VASP using the PBE[11] exchange-correlation functional and a plane-wave basis set to further understand the anisotropy of charge transport in single crystal **1** and **2**. The band structure calculations were based on the optimized crystal structure. Fig. 4 depicts the electronic band structure along with high symmetry directions and Table-5 listed the detailed bandwidths of valence band and conduction band along different directions. The results show that the electronic band structures of crystal **1** and **2** are similar, which is attributed to similar molecular structure and stacking arrangements in the crystal. Compounds **1** and **2** are indirect-gap semiconductors and they possess a band gap of 0.65 and 0.46 eV, respectively, with valence band maximum at X point and conduction band minimum at Γ point. The valence band and conduction band show noticeable dispersion, thus suggests that compounds **1** and **2** could be used as ambipolar transport material. For valence band, the big dispersion is observed along the symmetry line between Γ and X, which correspond to a axis in real space. In the hopping model, the pathway 3 of compounds **1** and **2** with the biggest hole transfer integral are also along this direction. For conduction band, the directions along the symmetry line between T and Γ, Γ and X, Y and Γ have the largest dispersions than any other ones. From the discussion on the transfer integral, pathway 2 of compounds **1** and **2** along b axis with the biggest electron transfer integral

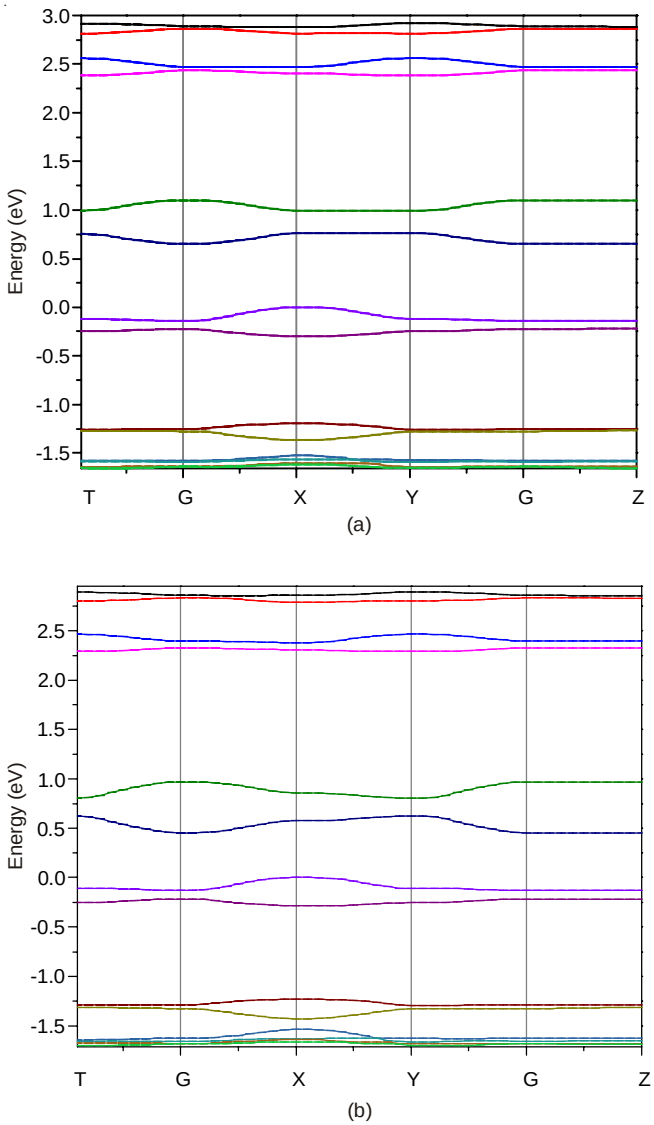

Fig. 4. Band structures of the crystal **1** (a) and **2** (b). Monoclinic space group P-1. The energies are plotted along directions in the first Brillouin zone connecting the point: G = (0, 0, 0), X = (0.5, 0, 0), Y = (0, 0.5, 0), Z = (0, 0, 0.5), T = (0, 0.5, 0.5)

is corresponded to the YΓ direction in reciprocal space. Thus we can find that the directions with large dispersions in both valence band and conduction band were also present bigger transfer integrals in the hopping model. The results here are consistent with the analysis from transfer integral. In addition, most of the conduction band bandwidths for compound **2** show clearly bigger dispersion than that for compound **1**, especially along the YΓ direction. The electron transport behavior was determined by the energy dispersion degree at the bottom of the conduction band. The abundant dispersion of conduction band indicate strong electron carrier mobility. Thus compound **2** exhibit higher electron conductivity than compound **1**, which is agree well with the results by Marcus theory.

TABLE-5
BANDWIDTH OF VALENCE BAND (VB) AND CONDUCTION BAND (CB) ALONG DIFFERENT HIGH SYMMETRY LINES IN eV

	Compound **1**		Compound **2**	
	VB	CB	VB	CB
TΓ	0.022	0.101	0.018	0.166
ΓX	0.143	0.104	0.125	0.120
XY	0.123	0.000	0.108	0.048
YΓ	0.020	0.103	0.017	0.167
ΓZ	0.002	0.000	0.002	0.000

Conclusion

In summary, we have systematically investigated the structural, electronic and charge transport properties of **1** and **2**. The equilibrium geometries of the neutral, cationic and anionic states for compound were optimized by means of B3LYP methods at the 6-31+G** basis sets. The results indicates that geometrical modifications of compounds **1** and **2** are slight when the charge transfer takes place, resulting in small λ_h and λ_e. The introduction of Se atom can effectively reduce the reorganization energy, thus compound **2** shows smaller hole and electron reorganization energies as compared to compound **1**. The HOMO and LUMO of compounds **1** and **2** possess delocalized π-orbital features. The transfer integrals of compounds **1** and **2** are big and comparative with the biggest values in the range of 10^{-1} eV. The S···N and Se···N interaction is favorable to the LUMO electronic coupling between neighbors and plays a major role in the determination of the electron mobility of material. Calculated hole and electron mobilities suggest ambipolar charge transfer features of compounds **1** and **2**. Both from the viewpoint of band model and hopping model, compounds **1** and **2** are found to be good candidates for ambipolar semiconducting materials and have the potential application in organic optoelectronic devices.

REFERENCES

1. M. Bendikov, F. Wudl and D.F. Perepichka, *Chem. Rev*., **104**, 4891 (2004).
2. J.E. Anthony, *Chem. Rev*., **106**, 5028 (2006).
3. V. Coropceanu, J. Cornil, D.A. da Silva Filho, Y. Olivier, R. Silbey and J.L. Brédas, *Chem. Rev*., **107**, 926 (2007).
4. H. Minemawari, T. Yamada, H. Matsui, J. Tsutsumi, S. Haas, R. Chiba, R. Kumai and T. Hasegawa, *Nature*, **475**, 364 (2011).
5. C. Mitsui, T. Okamoto, H. Matsui, M. Yamagishi, T. Matsushita, J. Soeda, K. Miwa, H. Sato, A. Yamano, T. Uemura and J. Takeya, *Chem. Mater*., **25**, 3952 (2013).
6. M.X. Zhang and G.J. Zhao, *J. Phys. Chem. C*, **116**, 19197 (2012).
7. B.D. Lindner, B.A. Coombs, M. Schaffroth, J.U. Engelhart, O. Tverskoy, F. Rominger, M. Hamburger and U.H.F. Bunz, *Org. Lett*., **15**, 666 (2013).
8. S.S. Zhao, F. Yu, G.C. Yang, H.Y. Zhang, Z.M. Su and Y. Wang, *Dalton Trans*., **41**, 7272 (2012).
9. T.C. Jiang, Z.Y. Wang, B.B. Du and S.S. Zhao, *Chin. Chem. Lett*., **24**, 945 (2013).
10. R.A. Marcus, *Rev. Mod. Phys*., **65**, 599 (1993).
11. J.P. Perdew, K. Burke and M. Ernzerhof, *Phys. Rev. Lett*., **77**, 3865 (1996).